Electron Vortex Dynamics and Two-Dimensional Field Analysis

K. Ito*, A. Sanpei* and Y. Kiwamoto†

*Graduate School of Human and Environmental Studies, Kyoto University, Sakyo-ku, Kyoto 606-8501, Japan
†Department of Fundamental Science, Integrated Human Studies, Kyoto University, Kyoto 606-8501, Japan

Abstract. In recent paper [K. Ito, *et al.*, Jpn. J. Appl. Phys. **40**, 2558 (2001)], we present a fast and sufficiently accurate procedure to construct the potential and the electric field distribution from the observed electron density distribution in two-dimensional plane. Using this procedure, we obtain quantitative agreement between the observed velocity of the clump motion and the calculated velocity of that determined by the field analysis. In addition, the strong deformation of the clump is observed when that moves in the shear of the background vortex.

INTRODUCTION

The dynamics of a nonneutral electron plasma that is strongly magnetized and homogeneous along the magnetic field is equivalent with the two-dimensional (2D) Euler fluid [1, 2]. The correspondence between the electron density $n(x,y)$ and the vorticity $\zeta(x,y)$ and that between the electric potential $\phi(x,y)$ and the stream function $\psi(x,y)$ eases the diagnostics and analyses of the electron vortex motion compared with those for neutral fluid vortices. The 2D structures of the density (vorticity) distribution is determined experimentally in terms of the luminosity distribution of electrons collected on a phosphor screen that serves also as a collector of the total charge to determine the total number of electrons [3, 4].

From the observed 2D density distribution, we determine the electrostatic potential and electric field distribution in the 2D plane by employing Fourier-Bessel series expansion of the observed density distribution for fast numerical processing [4]. The potential distribution $\phi(x,y)$ conforms to the stream function $\psi(x,y)$ in terms of fluid dynamics, so that many aspect of fluid dynamics can be presented in the language of electromagnetism. This fast numerical analysis is essential for detailed and extensive studies of vortex dynamics or turbulence.

We have experimentally observed radial oscillations in the trajectory of a clump of a vorticity moving up the slope of the background vorticity distribution [3]. This oscillation is not expected from the linear theory [5], and we were led to the interpretation that the main mechanism responsible for the oscillations is the azimuthal electric field associated with the differential rotation of the perturbed density distribution in the background behind the clump [3].

CP606, *Non-Neutral Plasma Physics IV*, edited by F. Anderegg et al.

Using this field analysis, we have obtained quantitative agreement between the observed speed of the oscillation and the calculated speed determined by the field analysis. It also demonstrates the influence of structures in the background vortex on the dynamics of coherent vortices [6, 7, 8, 9]. On the other hand, it is observed that the clump is stretched in the background vortex shear along the stream function. There is a possibility that it also influences the vortex motion.

The experiment is carried out with the Malmberg trap. The details of the experimental configuration have been reported in refs. 3 and 4.

DERIVATION OF POTENTIAL FIELD FROM OBSERVED DENSITY DISTRIBUTION[4]

In the Malmberg trap configuration, the magnetic field $\mathbf{B}_0$ is homogeneous and the axial distribution of the vacuum-field potential ϕ^v is flat in the trap region. Therefore, we can safely approximate that the chord-averaged density $n(x,y) = n_l(x,y)/L$ represents the actual density distribution of the electrons. Here, L is the axial length of the trap region expected from ϕ^v. Because L is much larger than the transverse dimension of the electron density distribution, we can introduce a 2D analysis for determining the potential distribution in the main part of the trapped region by neglecting the effects from the ends [4].

The potential distribution generated by the electrons is given in a 2D form $\phi(r,\theta)$ that satisfies the Poisson's equation.

$$\left(\frac{1}{r}\frac{\partial}{\partial r}r\frac{\partial}{\partial r}+\frac{1}{r^2}\frac{\partial^2}{\partial^2\theta}\right)\phi(r,\theta)=\frac{e}{\varepsilon_0}n(r,\theta). \tag{1}$$

The contribution of the conducting wall surrounding the plasma enters as a boundary condition $\phi(R,\theta)=0$ at the wall of a radius R.

First, we Fourier-expand Poisson's equation in the azimuthal angle θ to obtain a set of ordinary differential equations in the radial coordinate r. $\phi_m^{c,s}(r)$ and $n_m^{c,s}(r)$ are the mth Fourier component of the potential and the density, respectively. The density part $n_m^{c,s}(r)$ are calculated from the observed CCD images. We further expand $n_m^{c,s}(r)$ in a series of Bessel functions $J_m(z)$ to determine the associated terms of the potential that is obtained as,

$$\begin{aligned}\phi(r,\theta) &= \frac{e}{2\varepsilon_0}\sum_{n=1}^{\infty}\beta_{0n}^{c}J_0\left(\frac{\chi_{0n}}{R}r\right)\\ &+ \frac{e}{\varepsilon_0}\sum_{m=1}^{\infty}\left\{\cos m\theta\sum_{n=1}^{\infty}\beta_{mn}^{c}J_m\left(\frac{\chi_{mn}}{R}r\right)+\sin m\theta\sum_{n=1}^{\infty}\beta_{mn}^{s}J_m\left(\frac{\chi_{mn}}{R}r\right)\right\},\end{aligned} \tag{2}$$

where $J_m(\chi_{mn})=0$ with $n=1,2,3,....$, and

$$\beta_{mn}^{c,s}=-\frac{2}{\{\chi_{mn}J_{m+1}(\chi_{mn})\}^2}\int_0^R dr\,r\,J_m\left(\frac{\chi_{mn}}{R}r\right)n_m^{c,s}(r).$$

Here the upper limit of the azimuthal mode number m_{max} and the radial mode number n_{max} are taken as $m_{max} = 100$ and $n_{max} = 100$. The calculation of the potential requires about 1 min. on a personal computer. Once the potential distribution $\phi(r,\theta)$ is constructed, the electric field can be determined from $\phi(r,\theta)$.

Similarly, we can also reconstruct the density profile if we remove the constant e/π and replace the coefficients $\beta_{mn}^{c,s}$ with $\alpha_{mn}^{c,s} = -(\chi_{mn}/R)^2\beta_{mn}^{c,s}$ in eq. (2). The discrepancy Δ_e between the original density profile n_o and the reconstructed profile n_{FB} may be defined as

$$\Delta_e = \frac{\sqrt{\Sigma(n_{FB} - n_o)^2}}{\Sigma n_o} \tag{3}$$

by summing all the pixels. In most cases, Δ_e is found to be less than 1%.

DYNAMICS OF A CLUMP IN THE BACKGROUND VORTEX

In this section, we show an experimentally observed dynamics of a clump in a background vorticity distribution. In our experiments, generally, the radius of the clump is very small compared with that of the background vortex, and the circulation Γ_c of clump is less than a few percent of Γ_b. The circulation Γ is proportional to the electron number N. However, the vorticity of the clump ζ_c is ten times as high as that of the background vortex ζ_b. Accordingly, we can assume the clump as the strong point vortex in our experiments.

Figures 1 show typical time evolution of the 2D vorticity distribution. Here, the electron number of the clump and background vortex is $N_c = 1.2 \times 10^7$ and $N_b = 1.9 \times 10^8$, respectively. The upper panels are total vorticity distribution $\zeta(x,y,t)$ observed

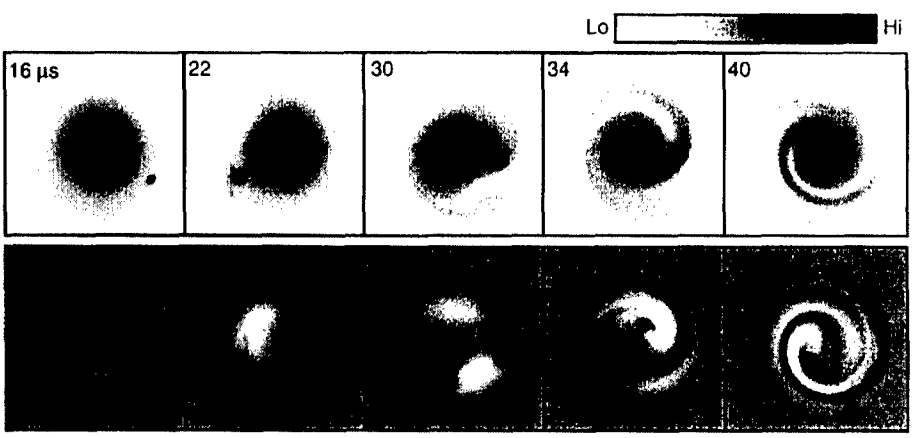

FIGURE 1. Time evolution of 2D vorticity distribution. The upper panels show the total vorticity distribution observed with CCD camera . The lower panels show the perturbed part of the background vortex from the initial background vortex distribution.

with CCD camera. It is observed that the clump climbs up the background vorticity gradient as it rotates creating a spiral streak behind it.

The lower panels show the perturbed part of the background vortex distribution $\delta\zeta_b(x,y,t)$ which is determined by subtracting the initial background distribution $\zeta_b(x,y,0)$ from each distribution $\zeta(x,y,t)$ in the upper panels. It is observed that the negative (positive) perturbation in front (behind) of the clump. It is considered that this deformation of the background vortex generates the radial electric field, and the $\mathbf{E} \times \mathbf{B}$ drift caused by this field drive the radial motion of the clump.

ANALYSIS OF THE CLUMP DYNAMICS

Figure 2(a) shows the radial distance r_c of a clump from the center of the background vorticity against the time with different circulation of clumps ($N_c = (2.4 - 6.3) \times 10^6$) when the background vorticity profile is fixed ($N_b = 1.9 \times 10^8$). The clump begins its free motion at 15 μs on disconnection from the electron source. Solid lines represents radial distance calculated from the Schecter's theoretical model [5] using the full experimental parameters of the initial distribution. The experimentally observed orbit of the clump is in almost agreement with the orbit obtained from the theoretical model. In the experiment, however, we can observe the oscillation of the orbit of the clump motion. We consider that the oscillation of the orbit is driven by the azimuthal electric field caused by the strong deformation of the background vortex [3].

Figure 2(b) shows the radial velocity of the clump motion in the case indicated by open triangles in Fig. 2(a). The open triangles represent the radial velocity calculated from the observed radial distance of the clump. The closed triangles indicate the radial velocity driven by $\mathbf{E} \times \mathbf{B}$ drift when the electric filed acting on the clump is calculated with the field analysis. The solid line represents the radial velocity calculated form the

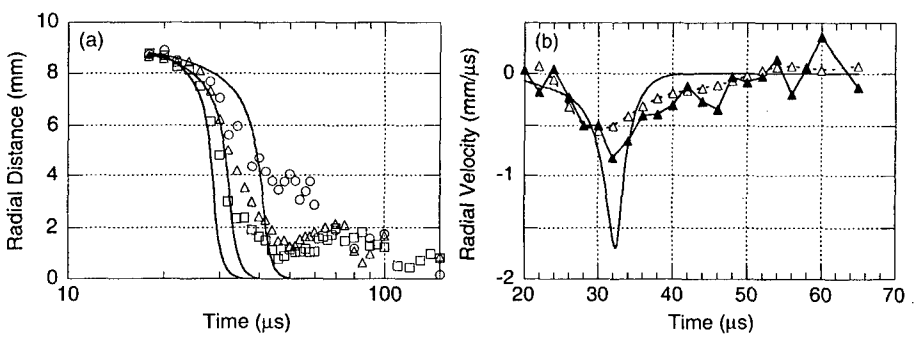

FIGURE 2. (a) The symbols are indicate the observed radial distance r_c of the clump from the center of the background vortex for different $N_c/10^6 = 2.4(\bigcirc), 4.1(\triangle), 6.3(\square)$. Solid lines represents the radial distance calculated from the Schecter's theoretical model. (b) Radial velocity of the point vortex in the case of $N_c = 4.1 \times 10^6$ in Fig. 2(a). Open triangles represent the directly observed velocity from observed vorticity distribution and closed triangles indicate the velocity calculated with the field analysis method. Solid line shows the velocity expected from the theoretical model.

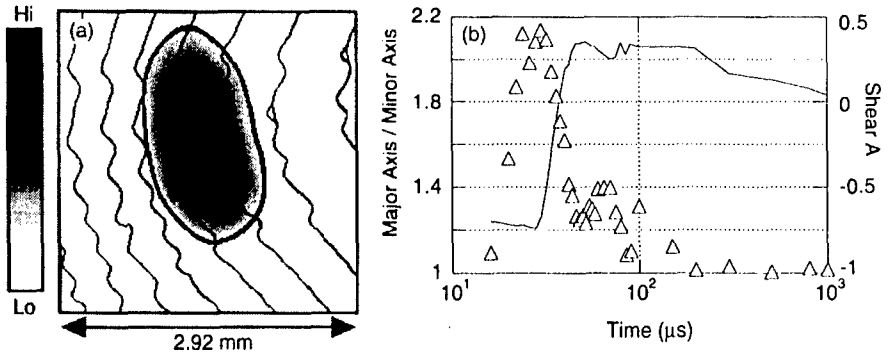

FIGURE 3. (a) Typical image of a clump stretched with the shear of the background vortex at t = 30 μs. Thin lines represent the stream function. Thick line indicates the 1/e contour of the vorticity. (b) Open triangles represent the ratio of the major axis to minor axis. The solid line indicates the shear of the background vortex.

theoretical model.

The radial velocity calculated with the field analysis is in good agreement with the observed velocity. It is noticed that the reverse of the radial velocity is reproduced from the field analysis. Therefore, we actually confirm the reverse of the radial velocity driven by the $\mathbf{E} \times \mathbf{B}$ drift by the field analysis. It indicates that this fast numerical analysis is essential for detailed and extensive studies of vortex dynamics.

It is observed that the maximum velocities calculated from the experimental data are slow compared with the theoretical value. We also consider that it originates in a strong deformation of the background vortex and that of the clump mentioned below.

We examine the influence which the background vortex exerts on the clump. Figure 3(a) shows the typical vorticity distribution around the clump in the background vortex. Thin lines represent the stream function and thick line indicates the 1/e contour of the clump vorticity. It is observed that the clump is stretched along the stream function.

Figure 3(b) plots the ratio a of the major axis to minor axis of the clump ($\triangle$) and the rotation shear $A = -rd\Omega_b/dr$ of the background vortex (solid line) as a functions of the time. Here, $\Omega_b(r)$ is the angular frequency of rotation of the background vortex. The clump is round ($a \approx 1$), immediately after the free motion of clump starts. After that, the clump is stretched swiftly along the stream function. The clump is stretched most ($a \approx 2.2$) at t = 30 μs when the shear A of the background vortex is strongest and the radial velocity of the clump is fastest as shown in Figs. 3(b) and 2(b). When the clump approaches the center of the background vortex, the shear A of the background vortex becomes weak and the clump rounds again. It is confirmed that a clump is stretched with a shear of a background vortex.

In a numerical simulation of neutral fluid, it has been considered that the deformation of the vortex is very important to the merging between vortices [10]. We have reported that the merging between the clumps is accelerated in the background vortex. On the other hand, we have observed that two clumps continue to revolve around each other with a fixed distance though they approach in close distance in the background vor-

tex [7]. We consider that the clump dynamics and the interaction between these in the background vortex are controlled by not only the transformation of the background vortex but also the clump deformation caused by the interaction between the clump and the background vortex.

CONCLUSIONS

We have developed a fast procedure to numerically construct the 2D field distribution from the observed image data directly related to the electron density distribution. We have examined the dynamics of the clump in the background vorticity distribution using this field analysis. As a result, we have obtained the quantitative agreement between the observed velocity of the clump motion and the calculated velocity determined by the field analysis. It includes the oscillation of the clump orbit. It is consider that this method is useful for extensive studies of vortex dynamics or turbulence.

We also examine the deformation of the clump. It is observed that the clump which has the strong vorticity is stretched in the background shear. We have considered that the clump deformation caused by the background vortex shear plays a role as important as the background vortex deformation in the dynamics of a clump and interaction between these in the background vortex.

ACKNOWLEDGMENTS

The authors thank Prof. A. Mohri for stimulating discussion. This work was supported by a Grant-in-Aid from the Ministry of Education, Science, Sports and Culture and by the collaborative research program of National Institute for Fusion Science.

REFERENCES

1. Levy, R. H., Phys. Fluids **11**, 920 (1968).
2. Fine, K. S., Driscoll, C. F., Phys. Rev. Lett. **74**, 4424 (1995).
3. Kiwamoto, Y., Ito, K., Sanpei, and A., Mohri, A., Phys. Rev. Lett. **85**, 3173 (2000).
4. Ito, K., Kiwamoto, Y., and Sanpei, A., Jpn. J. Appl. Phys. **40**, 2558 (2001).
5. Schecter, D. A., and Dubin, D. H. E., Phys. Rev. Lett. **83**, 2191 (1999).
6. Jin, D. Z. and Dubin, D. H. E., Phys. Rev. Lett. 80, 4434 (1998).
7. Kiwamoto, Y., Ito, K., Sanpei, A., Mohri, A., Yuyama, T., and Michishita, T., J. Phys. Soc. Jpn. (Letter) **68**, 3766 (1999).
8. Sanpei, A., Kiwamoto, Y., and Ito, K., J. Phys. Soc. Jpn. (Lett.) **70**, No.10(2001).
9. Kiwamoto, Y., Ito, K., Sanpei, A., et al. reported in this workshop.
10. Melander, M.V., Zabusky, N.J. and Mcwilliams, J.C., J. Fluid Mech. **195**, 303 (1988).